

AD-764 059

HYPersonic, TURBuLENT, COLD-WALL,
SKIN-FRICTION AND HEAT-TRANSFER
MEASUREMENTS ON AN AXISYMMETRIC
SHARP CONE

Kuei-Yuan Chien

Naval Ordnance Laboratory
White Oak, Maryland

15 June 1973

DISTRIBUTED BY:



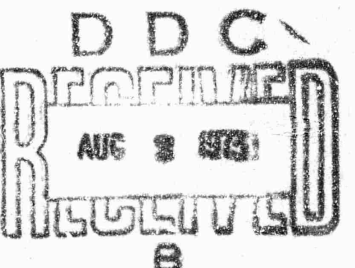
National Technical Information Service
U. S. DEPARTMENT OF COMMERCE
5285 Port Royal Road, Springfield Va. 22151

AD 764059

HYPersonic, TURBuLENT, COLD-WALL,
SKIN-FRiction AND HEAT-TRANSFER
MEASUREMENTS ON AN AXISYMMETRIC
SHARP CONE

BY
Kuei-Yuan Chien

15 JUNE 1973



NOL

NAVAL ORDNANCE LABORATORY, WHITE OAK, SILVER SPRING, MARYLAND

APPROVED FOR PUBLIC RELEASE; DISTRIBUTION UNLIMITED

NOLTR 73-108

NATIONAL TECHNICAL
INFORMATION SERVICE

R33

UNCLASSIFIED

Security Classification

DOCUMENT CONTROL DATA - R & D

(Security classification of title, body of abstract and indexing annotation must be entered when the overall report is classified)

1. ORIGINATING ACTIVITY (Corporate author)		2a. REPORT SECURITY CLASSIFICATION UNCLASSIFIED	
Naval Ordnance Laboratory White Oak, Silver Spring, Maryland 20910		2b. GROUP N/A	
3. REPORT TITLE HYPersonic, TURBULENT, COLD-WALL, SKIN-FRICTION AND HEAT-TRANSFER MEASUREMENTS ON AN AXISYMMETRIC SHARP CONE			
4. DESCRIPTIVE NOTES (Type of report and inclusive dates)			
5. AUTHOR(S) (First name, middle initial, last name) Kuei-Yuan Chien			
6. REPORT DATE 15 June 1973		7a. TOTAL NO OF PAGES 30 ⁸³	7b. NO. OF REFS 28
8. CONTRACT OR GRANT NO.		9a. ORIGINATOR'S REPORT NUMBER(S) NOLTR 73-108	
b. PROJECT NO. ORD 035A-001/092-1/UF-32 322-502		9b. OTHER REPORT NO(S) (Any other numbers that may be assigned to this report)	
10. DISTRIBUTION STATEMENT Approved for public release; distribution unlimited			
11. SUPPLEMENTARY NOTES		12. SPONSORING MILITARY ACTIVITY Naval Ordnance Systems Command Washington, D. C. 20361	
13. ABSTRACT Turbulent skin-friction coefficients directly measured on an axisymmetric five-degree-half-angle sharp cone by two floating-element skin-friction balances at a free-stream Mach number of 7.9 are presented. Heat-transfer distributions are obtained simultaneously. These results yield directly the Reynolds analogy factor. Experimental data are used to evaluate the predictive methods of Van Driest, Spalding and Chi, Sommer and Short, and Clark and Creel. On the basis of measured skin-friction coefficients, which covered a range of wall-to-stagnation temperature ratios (T_w/T_0) of 0.24 to 0.41 and Reynolds numbers at the location of the skin-friction balance of 1.45×10^7 to 2.16×10^7 , we conclude that the method of Van Driest and that of Clark and Creel predict the measurements within about 10 percent, whereas the methods of Spalding and Chi and Sommer and Short underpredict the data by about 30 and 20 percent, respectively. Except for the relatively low-Reynolds-number case, the directly measured sharp-cone Reynolds analogy factor is between 1.01 and 1.07, which is in good agreement with the recent flat-plate measurements of Keener and Polek. Finally, results indicate that the Stanton Number is essentially constant for T_w/T_0 between 0.20 and 0.36, whereas it decreases by about 10 percent at $T_w/T_0 = 0.11$.			

UNCLASSIFIED

Security Classification

14 KEY WORDS	LINK A		LINK B		LINK C	
	ROLE	WT	ROLE	WT	ROLE	WT
hypersonic turbulent flow skin-friction data heat-transfer data Reynolds analogy factor axisymmetric sharp cone						

HYPersonic, TURBULENT, COLD-WALL, SKIN-FRICTION
AND HEAT-TRANSFER MEASUREMENTS ON AN
AXISYMMETRIC SHARP CONE

Prepared by:
Kuei-Yuan Chien

ABSTRACT: Turbulent skin-friction coefficients directly measured on an axisymmetric five-degree half-angle sharp cone by two floating-element skin-friction balances at a free-stream Mach number of 7.9 are presented. Heat-transfer distributions are obtained simultaneously. These results yield directly the Reynolds analogy factor. Experimental data are used to evaluate the predictive methods of Van Driest, Spalding and Chi, Sommer and Short, and Clark and Creel. On the basis of measured skin-friction coefficients, which covered a range of wall-to-stagnation temperature ratios (T_w/T_0) of 0.24 to 0.41 and Reynolds numbers at the location of the skin-friction balance of 1.45×10^7 to 2.16×10^7 , we conclude that the method of Van Driest and that of Clark and Creel predict the measurements within about 10 percent, whereas the methods of Spalding and Chi and Sommer and Short underpredict the data by about 30 and 20 percent, respectively. Except for the relatively low-Reynolds-number case, the directly measured sharp-cone Reynolds analogy factor is between 1.01 and 1.07, which is in good agreement with the recent flat-plate measurements of Keener and Polek. Finally, results indicate that the Stanton number is essentially constant for T_w/T_0 between 0.20 and 0.36, whereas it decreases by about 10 percent at $T_w/T_0 = 0.11$.

NAVAL ORDNANCE LABORATORY
WHITE OAK, MARYLAND

NOLTR 73-108

15 June 1973

HYPERSONIC, TURBULENT, COLD-WALL, SKIN-FRICTION AND HEAT-TRANSFER
MEASUREMENTS ON AN AXISYMMETRIC SHARP CONE

This report presents results of skin-friction and heat-transfer measurements obtained directly on an axisymmetric five-degree half-angle sharp cone at a free-stream Mach number of 7.9. Comparisons with the predictive schemes of Van Driest, Spalding and Chi, Sommer and Short, and Clark and Creel are also included. Except for the relatively low-Reynolds-number case, the measured sharp-cone Reynolds analogy factor is close to the classical value of unity and is in good agreement with the recent flat-plate measurements. For the range of wall-to-stagnation temperature ratios covered in the tests, the method of Van Driest and that of Clark and Creel predict the measured skin friction within about 10 percent, whereas the other two methods underpredict the data considerably more. Heat transfer proves to be relatively insensitive to wall-temperature changes.

The author wishes to extend his thanks to Mr. S. Sacks (Exchange Scientist from Naval Ship Research and Development Center) for his assistance in reducing the data and his development of a computer program for theoretical predictions, and to his colleague, Mr. R. Hall, at NOL, for many helpful discussions.

Present study was supported by Naval Ordnance Systems Command under Task Number ORD 035A-001/092-1/UF-32-322-502.

ROBERT WILLIAMSON II
Captain, USN
Commander

L. H. Schindel
L. H. SCHINDEL
By direction

CONTENTS

	Page
INTRODUCTION.....	1
SYMBOLS.....	2
APPARATUS AND TEST.....	3
DATA REDUCTION.....	4
PREDICTIVE METHODS.....	5
RESULTS AND DISCUSSION.....	7
CONCLUSIONS.....	8
REFERENCES.....	9

TABLES

Table	Title
1	Thermocouple Locations and the Model-Skin Thickness
2	Test Conditions and Skin-Friction Data

ILLUSTRATIONS

Figure	Title
1	Schematic of the Model
2	Constant-Pressure Specific Heat Capacity of Armco 17-4 PH Stainless Steel
3a	Skin-Friction Balance and the Model
3b	Front View of the Skin-Friction Balance
3c	Back View of the Skin-Friction Balance
4	Calibration Results of Skin-Friction Balances
5	Comparison of Skin-Friction Data with Theories
6a	Stanton Number Distribution; $T_w/T_o = 0.35$
6b	Stanton Number Distribution; $T_w/T_o = 0.32$
6c	Stanton Number Distribution; $T_w/T_o = 0.24$
6d	Stanton Number Distribution; $T_w/T_o = 0.20$
6e	Stanton Number Distribution; $T_w/T_o = 0.11$
7	Wall-Temperature Effect on the Stanton Number
8	Reynolds Analogy Factor

INTRODUCTION

Recently, there has been considerable interest in studying hypersonic, turbulent boundary-layer flows at low-wall temperatures. This is undoubtedly due to their significance in the optimal design of re-entry vehicles useful for defense and space applications. From an engineer's point of view, the desired goal of such a study is to establish the usefulness of a predictive scheme which is both simple and accurate. In this respect, we might mention the rather extensive study of Spalding and Chi (Ref. (1)), who compared 20 methods with a large number of directly and indirectly measured flat-plate skin-friction data. Subsequently, heat-transfer data on cones and heat-transfer and skin-friction data on flat plates and nozzle walls have been used by various investigators to evaluate different theories (Refs. (2) through (13)). Conclusions from these studies may be summarized as follows:

1. The methods of Van Driest (Ref. (14)) and Coles (Ref. (15)) predict skin friction within about 10 percent of experimental flat-plate and tunnel-wall data for $T_w/T_{\infty} > 0.3$ (Refs. (8), (10), and (11)).

2. For $T_w/T_{\infty} \sim 0.15$, results obtained from the method of Spalding and Chi (Ref. (1)) agree reasonably well with the skin-friction measurements obtained in a shock tunnel (Ref. (4)).

3. Evaluation of theories for heat-transfer predictions depends critically on the accepted value of the Reynolds analogy factor. However, a recent survey conducted by Cary (Ref. (16)) indicates a definite need for more systematic studies on the subject.

4. The effect of wall temperature on measured heat-transfer rate is still not yet settled. For example, results of Cary (Ref. (17)) indicate little influence for $0.2 \leq T_w/T_{\infty} \leq 0.7$, whereas Drougge (Ref. (18)) and Wilson (Ref. (7)) both suggest a rather large decrease in the Stanton number for $T_w/T_{\infty} \gtrsim 0.2$.

It is therefore clear that there is still a great need for simultaneously measured skin-friction and heat-transfer data obtained at low-wall temperatures. Furthermore, directly measured skin-friction coefficients on pointed axisymmetric bodies, which are of great technical interest, appear to be quite limited. For example, Wilson (Ref. (7)) deduced average skin-friction coefficients on a sharp cone from measurements of total drag and pressure distribution. Local skin-friction coefficients could be inferred only when additional assumptions such as the functional dependence of the local skin-friction coefficient on distance were made. A completely new approach has been taken in the present study. The purpose of this report is to present turbulent skin-friction coefficients directly measured on an axisymmetric five-degree half-angle sharp cone by two floating-element skin-friction balances designed and constructed at NOL. In addition, heat-transfer

measurements are obtained simultaneously. Therefore, the Reynolds analogy factor is directly determined. These sharp-cone results will be used to compare with the existing data of the Reynolds analogy factor obtained on flat plates. Furthermore, the effect of wall temperature on the Stanton number will be presented. Finally, comparisons with the predictive schemes of Spalding and Chi (Ref. (1)), Van Driest (Ref. (14)), Sommer and Short (Ref. (19)) and Clark and Creel (Ref. (20)) will also be made.

SYMBOLS

c_f	local skin-friction coefficient, $\tau_w / \frac{1}{2} \rho_e U_e^2$
c_p	specific heat at constant pressure
h	heat-transfer coefficient, $\dot{q}_w / (T_{aw}-T_w)$
M	Mach number
p	pressure
\dot{q}_w	convective heat-transfer rate to the surface per unit area
r	recovery factor
Re/L	unit Reynolds number, $\rho_e U_e / \mu_e$, ft^{-1}
Re_x	Reynolds number, $\rho_e U_e x / \mu_e$
$Re_{x'}$	Reynolds number based on x' , $\rho_e U_e x' / \mu_e$
Re_θ	Reynolds number based on the momentum thickness, $\rho_e U_e \theta / \mu_e$
S_t	Stanton number, $\dot{q}_w / \rho_e U_e C_p (T_{aw}-T_w)$
t	time
T	absolute temperature
U	velocity
x	distance along surface from the cone tip
x'	distance along surface from the virtual origin of turbulent flow
δ_m	model skin thickness
θ	momentum thickness
μ	coefficient of viscosity

p	density
t	shear stress
($\bar{}$)	variable transformed to the equivalent constant-flow-property case

Subscripts

aw	adiabatic wall
e	boundary-layer edge
EXP	experimental
m	model
THE	theoretical
w	wall
o	stagnation condition
∞	free-stream condition

APPARATUS AND TEST

The experimental investigation was conducted in the NOL Hypersonic Tunnel at a free-stream Mach number of 7.9 in air. A sharp, sting-supported, five-degree half-angle cone was used for the test. This combination of free-stream Mach number and cone half-angle yielded a local Mach number of 7.15 at the edge of the boundary layer. The model was made of Armco 17-4 PH stainless steel and was equipped with four pressure taps (for model alignment), two floating-element skin-friction balances and 40 thermocouples. A sketch of the cone together with some pertinent dimensions is shown in Figure 1.

A cooling box was used to control the surface temperature of the model. Liquid nitrogen, liquid CO₂, and compressed air (heated or unheated) were employed in the investigation to obtain a rather wide range of wall-to-stagnation temperature ratios. Two thermocouples were used to measure the surface temperature of the floating elements of the skin-friction balances. Two other thermocouples were located at the flexures of the two balances. A casing made of epoxy, nylon bolts, and insulating materials were used to shield the flexures, the moment arms and the linear variable differential transformers of the balances from conduction and radiation exchanges during severe cooling or heating periods. The transient-thin-wall technique was used to measure the heat-transfer rate. Thirty-six thermocouples were distributed along four rays on the model. The skin thickness of the model, δ_m , and the location of the thermocouples are listed in Table 1.

During a test, the model was first lowered into the cooling box. To protect the skin-friction balances, a lock was applied to hold them in position. The tunnel pressure was then reduced and the coolant introduced into the cooling box. Except for the case of liquid-nitrogen cooling, the air flow could first be established. The coolant was then shut off when the desired wall temperature had been reached. The lock was released for taking a tare reading, and then the balances relocked and the model quickly injected into the air stream. Liquid nitrogen solidifies for pressure below 94 torrs. Consequently, for this case we had to shut off the coolant before the tunnel pressure could be pulled further down from about 100 torrs to the desired level to establish the flow. Aluminum foil was used to avoid any accumulation of solid CO₂ on the model surface during cooling. Visual inspection through the tunnel window was routinely done to ensure no frost formation on the model surface. Data such as the voltage output from the linear-variable-differential transformers of the skin-friction balances, the thermocouples, the balance-lock indicator, and the potentiometer indicating the position of the injecting system were recorded on the NOL Data Acquisition and Recording Equipment System (DARE II). There are ten channels and ten scans available on DARE II. However, to reduce the time interval between two successive recordings of the voltage output from an instrument, only three scans of each channel were employed. Therefore, some of the thermocouples were connected instead to an oscilloscope (Midwestern). This information is also listed in Table 1. Test time is typically about 10 seconds. The test conditions are summarized in Table 2.

DATA REDUCTION

HEAT TRANSFER

The recorded temperature history of the model wall was used in the well-known transient-thin-wall technique to obtain the heat-transfer data. To utilize the technique, we need, in addition, to know the density, ρ_m, and the specific heat, C_{pm}, of the model-wall material. For stainless steel, the density was taken to be constant at 490.75 lbm/ft³. The specific heat was measured for us by the University of Massachusetts and the results are shown in Figure 2. Calculation indicates that errors due to normal conduction through the thin skin of the model are negligible. At each thermocouple location, a least-squares, second-degree polynomial fit to 16 successive temperature readings was employed to calculate the derivative of the wall temperature with respect to time, ∂T_w/∂t. A history of measured heat-transfer coefficient, h_m, was obtained from the relation

$$h_m = \frac{\rho_m C_{pm} \delta_m}{(T_{aw} - T_w)} \frac{\partial T_w}{\partial t} \quad (1)$$

The Thomas-Fitzsimmons initial-lateral-conduction-correction method (Ref. (21)) was then applied to this data block to yield a heat-transfer coefficient at time zero, the time at which aerodynamic heating began. Ten such data blocks consecutive in time and the corresponding heat-transfer coefficients at time zero, $h_a(0)$, were generated. When the variation in $h_a(0)$ from several consecutive data blocks was small, their average was selected to be the proper value. Repeated applications of the same process at different locations on the model then produced the desired heat-transfer distribution. The method was checked with two low-supply-pressure runs and good agreement with the well-known laminar boundary-layer theory was obtained in both cases. Additional confirmation may be found in the Results and Discussion, where agreement between data (before transition occurs) and the laminar theory is again good. The estimated accuracy of the heat-transfer data is about ± 5 percent.

SKIN FRICTION

A simulator was used to install the two skin-friction balances for bench-top calibrations. A picture showing the setup together with the model can be found in Figure 3. Typical calibration results are shown in Figure 4. Based on a least-squares linear fit, the balances proved to be linear within about 0.3 percent. An average of the repeated calibrations conducted between runs on site were used in the final data reduction. The surface area of the floating element is 0.441 in^2 . For every run, two tare readings were recorded, one before and one after the test. The result would be discarded if the difference between the two tare readings proved large. Some measurements were rejected because of other reasons. For example, there was a drastic difference (about a factor of 40) in wall thickness between the location of the skin-friction balance and the thin skin part of the model where heat transfer was measured. This made the maintenance of a uniform model-wall temperature even more difficult. In addition, a lock could be applied to hold the balances in position during the model-injection period. This avoided the inertial effect caused by the acceleration and deceleration of the injecting mechanism. However, the extent of the modification of the model-temperature distribution due to aerodynamic heating before the lock could be released manually was difficult to control. Several runs were conducted without the application of the lock. However, the initial transient effect on the skin-friction balances was quite large. Despite these difficulties, four runs yielded good skin-friction data, although the number of successful heat-transfer runs is almost three times as much. The skin-friction results are also listed in Table 2. The accuracy is estimated to be about ± 5 percent.

PREDICTIVE METHODS

LAMINAR FLOW

The well-known Blasius solution with Mangler transformation yields, for flow over a sharp cone, the relation

$$\bar{C}_f \approx \sqrt{3} \frac{0.664}{\sqrt{Re_x}} \quad (2)$$

The reference-temperature method of Rubesin and Johnson (Ref. (22)) can then be used to give

$$C_f = \sqrt{3} \frac{0.664}{\sqrt{Re_x}} \sqrt{\frac{T_e \mu^*}{T^* \mu_e}} \quad (3)$$

where the reference temperature is given by

$$T^* = T_e [1 + 0.032 M_e^2 + 0.58 (Tw/T_e - 1)] \quad (4)$$

The heat-transfer result is obtained by using the well-known formula of the Reynolds analogy factor for a laminar flow (Ref. (23))

$$\frac{2S_t}{C_f} = Pr^{-2/3} \quad (5)$$

and Equation (3). The Prandtl number is taken as constant, $Pr = 0.725$.

TURBULENT FLOW

In the interest of simplicity, the turbulent-flow methods of Spalding and Chi (Ref. (1)), Van Ories (Ref. (14)), Sommer and Short (Ref. (19)), and Clark and Creel (Ref. (20)) are considered. The incompressible formula of Karman and Schoenherr relating C_f to Re_θ (Ref. (10)) is used for predicting the compressible skin-friction coefficient from each of these methods. Since only surface properties were measured, the Reynolds number based on the momentum thickness is calculated from the momentum integral equation

$$\frac{C_f}{2} = \frac{dRe_\theta}{dRe_{x'}} + \frac{Re_\theta}{Re_{x'}} \quad (6)$$

The experimental results reported by Richards (Ref. (3)) suggest that the effective turbulent distance, x' , may be determined from the condition of matching the momentum thickness, θ , from a turbulent-flow theory to that of the laminar theory

at the midpoint of the transition zone. Calculations indicate that differences between this procedure and that where θ is matched at the end of the transition (as was suggested by Wallace, Ref. (4)) are (at the location of the skin-friction balance) about four percent for $Re_x \sim 15 \times 10^6$, and only about two percent for $Re_x \sim 22 \times 10^6$. Finally, Karman's formula for the Reynolds analogy factor as modified by Bertram and Neal (Ref. (2)) is used to calculate the heat-transfer predictions. Present data to be shown in the Section on Results and Discussion suggest $Re_x = 6 \times 10^6$ at the midpoint of transition. More details can be found in Reference (24).

RESULTS AND DISCUSSION

The comparison between the skin-friction measurements and the turbulent theories is shown in Figure 5. Present data cover a range of T_w/T_0 of 0.24 to 0.41 and Re_x of 1.45×10^7 to 2.16×10^7 . Results indicate that the methods of Van Driest, Sommer and Short, and Spalding and Chi underpredict the data by about 10, 20 and 30 percent, respectively, whereas the recently proposed reference-temperature method of Clark and Creel predicts the measurements within about ± 10 percent. These observations are in general agreement with the conclusions of other investigators whose results were obtained on flat plates and nozzle walls (Refs. (10), (11), and (20)).

Heat-transfer distributions along the cone surface for various wall-to-stagnation temperature ratios are depicted in Figure 6. The data exhibit the familiar picture of a laminar, then transitional and finally turbulent flow. Except for the case of the lowest T_w/T_0 ($= 0.11$), the agreement between the laminar solution and the data is quite good. This again confirms the general reliability of the testing technique and the data-reduction method for heat-transfer measurements. On the other hand, the degree of agreement between the turbulent data and the theories depends more strongly on T_w/T_0 . This dependence is better seen in Figure 7 for $Re_x = 2 \times 10^7$. Because of the scatter in the original data, a mean value for each run is used to construct the plot. In agreement with the results reported in References (5) and (7), the presently measured Stanton number is essentially constant for T_w/T_0 between 0.20 and 0.36. However, at $T_w/T_0 = 0.11$, there appears a decrease in the Stanton number by about ten percent. This is in the same trend as that reported by Drougge (Ref. (18)) and Wilson (Ref. (7)), although the decrease measured here is smaller. Because of the rapid change in the specific heat of the model material at very low temperatures (Fig. (2)), the present result at $T_w/T_0 = 0.11$ should be regarded as tentative. More systematic studies are required before a definitive conclusion can be reached.

As can be seen in Figure 7, none of the theoretical schemes considered here predicts the measured trend over the complete range of T_w/T_0 . However, the level of the prediction depends on the particular Reynolds analogy factor employed. For the conditions considered, the modified Karman's equation yields values between 1.10 to 1.14. With this form for the Reynolds analogy factor, the method of Van Driest predicts the data reasonably well for $T_w/T_0 > 0.2$. On the other hand, in agreement with Pearce (Ref. (9)), at $T_w/T_0 = 0.11$, only the method of Spalding and Chi gives a value that is within 10 percent of the measurement.

Finally, the Reynolds analogy factor as determined from the simultaneously measured skin-friction and heat-transfer data on the sharp-cone model is depicted in Figure 8. Also shown are the flat-plate results of Wallace (Ref. (4)), Neal (Ref. (25)), Keener and Polek (Ref. (26)), Holden (Ref. (27)), and that of Hironimus (Ref. (28)) as rereduced and tabulated by Cary (Ref. (16)). The symbol represents the average and the bar the variation at any given flow condition. The range of the Mach number included in Figure 8 is from 6.6 to 8.1. For edge Mach numbers of 5.9 to 7.7, Keener and Polek (Ref. (26)) found no distinct effects of Mach number on the Reynolds analogy factor. Despite this fact, a considerable amount of scatter among all the data is still present in Figure 8. Except for the relatively low-Reynolds-number case ($Re_x = 1.45 \times 10^7$ at $T_w/T_0 = 0.41$), the present sharp-cone data agree reasonably well with the flat-plate results of Keener and Polek, which suggest a value close to the classical limit of unity. Note that the rate of decrease of the Stanton number for $Re_x > 8 \times 10^6$ as shown in Figure 6a is distinctly faster for the lower total pressure runs (filled symbols). Whether this suggests a flow that is not yet fully turbulent is not clear. If no discrimination is applied to all of the data shown, Figure 8 suggests that the Reynolds analogy factor is independent of T_w/T_0 and equal to 1.1 which is quite close to the predictions given by the Karman's equation. Obviously, more systematic investigations, especially at low-wall temperature ratios, are definitely required.

CONCLUSIONS

Simultaneous measurements of skin friction and heat transfer directly measured on an axisymmetric sharp cone have been successfully obtained for an edge Mach number of 7.15 and for unit Reynolds numbers of 7.4×10^6 to 11×10^6 per foot. Several conclusions may be drawn. First of all, for T_w/T_0 between 0.24 and 0.41, both the method of Van Driest and that of Clark and Creel predict the skin-friction measurements within about ten percent. Utilizing the modified Karman's equation for the Reynolds analogy factor, the scheme of Van Driest gives reasonable predictions for $T_w/T_0 > 0.2$, whereas only the method of Spalding and Chi yields a value that is within 10 percent of the

measurement at $T_w/T_0 = 0.11$. In addition, the wall-temperature effect on the Stanton number proves to be quite small for T_w/T_0 above 0.2. If only the data at $Re_x \approx 2.2 \times 10^7$ are considered, present sharp-cone measurements of the Reynolds analogy factor are between 1.01 and 1.07, which agree very well with the flat-plate results of Keener and Polek. Finally, an examination of the present data and the results of the other investigators strongly suggests the need for more systematic studies for $T_w/T_0 \leq 0.2$.

REFERENCES

- (1) Spalding, D. B. and Chi, S. W., "The Drag of a Compressible Turbulent Boundary Layer on a Smooth Flat Plate with and without Heat Transfer," *Journal of Fluid Mechanics*, Vol. 18, Pt. 1, pp. 117-143, 1964.
- (2) Bertram, M. H. and Neal, L., Jr., "Recent Experiments in Hypersonic Turbulent Boundary Layers," *NASA TMX-56335*, 1965.
- (3) Richards, B. E., "Transitional and Turbulent Boundary Layers on a Cold Flat Plate in Hypersonic Flow," *Aeronautical Quarterly*, Vol. 18, pp. 237-258, 1967.
- (4) Wallace, J. E., "Hypersonic Turbulent Boundary-Layer Studies at Cold Wall Conditions," *Proc. 1967 Heat Transfer and Fluid Mechanics Institute*, pp. 428-451, 1967.
- (5) Bertram, M. H., Cary, A. M., Jr., and Whitehead, A. H., Jr., "Experiments with Hypersonic Turbulent Boundary Layers on Flat Plates and Delta Wings," *AGARD CP No. 30*, May 1968.
- (6) Perry, J. H. and East, R. A., "Experimental Measurements of Cold Wall Turbulent Hypersonic Boundary Layers," *AGARD CP No. 30*, May 1968.
- (7) Wilson, D. M., "A Correlation of Heat-Transfer and Skin-Friction Data and an Experimental Reynolds Analogy Factor for Highly Cooled Turbulent Boundary Layer at Mach 5.0," *NOLTR 69-51*, 1969.
- (8) Hopkins, E. J., Rubesin, M. W., Inouye, M., Keener, E. R., Mateer, G. C., and Polek, T. E., "Summary and Correlation of Skin-Friction and Heat-Transfer Data for a Hypersonic Turbulent Boundary Layer on Simple Bodies," *NASA TN D-5089*, 1969.
- (9) Pearce, B. E., "Comparison of Simple Turbulent Heating Estimates for Lifting Entry Vehicles," *Journal of Spacecraft*, Vol. 7, No. 10, pp. 1276-1278, 1970.
- (10) Hopkins, E. J. and Inouye, M., "An Evaluation of Theories for Predicting Turbulent Skin Friction and Heat Transfer on Flat Plates at Supersonic and Hypersonic Mach Numbers," *AIAA Journal*, Vol. 9, No. 6, pp. 993-1003, 1971.

- (11) Hopkins, E. J., Keener, E. R., Polek, T. E. and Dwyer, H. A., "Hypersonic Turbulent Skin-Friction and Boundary-Layer Profiles on Nonadiabatic Flat Plates," AIAA Journal, Vol. 10, No. 1, pp. 40-48, 1972.
- (12) Kemp, J. H., Jr. and Owen, F. K., "Nozzle Wall Boundary Layers at Mach Numbers 20 to 47," AIAA Journal, Vol. 10, No. 7, pp. 872-879, 1972.
- (13) Harvey, W. D. and Clark, F. L., "Measurements of Skin Friction on the Wall of a Hypersonic Nozzle," AIAA Journal, Vol. 10, No. 9, pp. 1256-1258, 1972.
- (14) Van Driest, E. R., "Problem of Aerodynamic Heating," Aeronautical Engineering Review, Vol. 15, No. 10, pp. 26-41, 1956.
- (15) Coles, D. E., "The Turbulent Boundary Layer in a Compressible Fluid," The Physics of Fluids, Vol. 7, No. 9, pp. 1403-1423, 1964.
- (16) Cary, A. M., Jr., "Summary of Available Information on Reynolds Analogy for Zero-Pressure-Gradient, Compressible, Turbulent-Boundary-Layer Flow," NASA TN D-5560, 1970.
- (17) Cary, A. M., Jr., "Turbulent Boundary-Layer Heat Transfer and Transition Measurements for Cold-Wall Conditions at Mach 6," AIAA Journal, Vol. 6, No. 5, pp. 958-959, 1968.
- (18) Drougge, G., "Measurements of Heat Transfer in a Highly Cooled Turbulent Boundary Layer at $M = 4.6$ and 7," FFA AU-120:4, Del II (Sweden), Apr 1965.
- (19) Sommer, S. C. and Short, B. J., "Free-Flight Measurements of Turbulent Boundary-Layer Skin Friction in the Presence of Severe Aerodynamic Heating at Mach Numbers from 2.8 to 7.0," Journal of the Aeronautical Sciences, Vol. 23, No. 6, pp. 536-542, 1956.
- (20) Clark, F. L. and Creel, T. R., Jr., "Reference Temperature Method for Predicting Turbulent Compressible Skin-Friction Coefficient," AIAA Journal, Vol. 11, No. 2, pp. 239-240, 1973.
- (21) Nagel, A. L., Fitzsimmons, H. D., and Doyle, L. B., "Analysis of Hypersonic Pressure and Heat-Transfer Tests on Delta Wings with Laminar and Turbulent Boundary Layers," NASA CR-535, Appendix A, Aug 1966.
- (22) Rubesin, M. W. and Johnson, H. A., "A Critical Review of Skin-Friction and Heat-Transfer Solutions of the Laminar Boundary Layer on a Flat Plate," ASME Trans., Vol. 71, No. 4, May 1949, pp. 385-388.

- (23) Hayes, W. D. and Probstein, R. F., "Hypersonic Flow Theory," Chap. VIII, pp. 294-298, Academic Press, New York, 1959.
- (24) Sacks, S., "Computation of the Skin Friction and Heat Transfer on a Sharp Cone in Axisymmetric Turbulent Hypersonic Flow," NOLTR /3-79, 12 Apr 1973.
- (25) Neal, L., Jr., "A Study of the Pressure, Heat Transfer and Skin Friction on Sharp and Blunt Flat Plates at Mach 6.8," NASA TN D-3312, 1966.
- (26) Keener, E. R. and Polek, T. E., "Measurements of Reynolds Analogy for a Hypersonic Turbulent Boundary Layer on a Nonadiabatic Flat Plate," AIAA Journal, Vol. 10, No. 6, pp. 845-846, 1972.
- (27) Holden, M. S., "Shock Wave-Turbulent Boundary Layer Interaction in Hypersonic Flow," AIAA Paper No. 72-74, 1972.
- (28) Hironimus, G. A., "Hypersonic Shock Tunnel Experiments on the W7 Flat Plate Model--Expansion Side, Turbulent Flow and Leading Edge Transpiration Data," CAL Report No. AA-1952-Y-2, Feb 1966.

TABLE 1
THERMOCOUPLE LOCATIONS AND THE MODEL-SKIN THICKNESS

Thermocouple Number	X, Inches	θ , Degrees	δ_m , Inches	Remarks
1	2	90	.0181	
2	3	180	.0177	
3	4	270	.0183	
4	5	0	.0194	
5	6	90	.0198	
6	6	180	.0191	On Midwestern
7	6	270	.0198	On Midwestern
8	6	0	.0204	On Midwestern
9	7	90	.0191	
10	8	180	.0194	
11	9	270	.0200	
12	10	0	.0200	On Midwestern
13	10	90	.0200	
14	10	180	.0202	On Midwestern
15	10	270	.0201	On Midwestern
16	12	0	.0224	
17	13	180	.0224	
18	14	90	.0226	
19	14	270	.0222	
20	15	0	.0225	
21	16	0	.0225	On Midwestern
22	16	90	.0223	
23	16	180	.0228	On Midwestern
24	16	270	.0226	
25	17	90	.0225	
26	18	0	.0222	
27	18	180	.0229	
28	19	270	.0224	
29	20	0	.0226	On Midwestern
30	20	90	.0226	
31	20	180	.0228	On Midwestern
32	20	270	.0224	On Midwestern
33	22	0	.0220	On Midwestern
34	22	90	.0218	Open During Test
35	22	180	.0218	
36	22	270	.0218	
37	23.44	90	-	At Surface of Balance 1
38	23.44	270	-	At Surface of Balance 2*
39	-	-	-	At Flexure of Balance 1
40	-	-	-	At Flexure of Balance 2

*Open During Test

TABLE 2
TEST CONDITIONS AND SKIN-FRICTION DATA

Run No.	P _o , psi	T _o , °R	10 ⁻⁶ Re/L, ft ⁻¹	T _w /T _o	C _f × 10 ³
18	2189	1440	11.07	.197	
19	2188	1437	11.07	.322	1.15
20	2183	1467	10.90	.194	
21	2186	1469	10.87	.351	1.21
23	2185	1495	10.46	.351	
24	2196	1471	10.88	.362	
26	1470	1442	7.40	.340	
27	1470	1443	7.40	.409	1.17
29	1481	1450	7.39	.366	
30	2188	1462	10.94	.108	
31	2191	1461	10.97	.242	1.26

UNCLASSIFIED
NOLTR 73-108

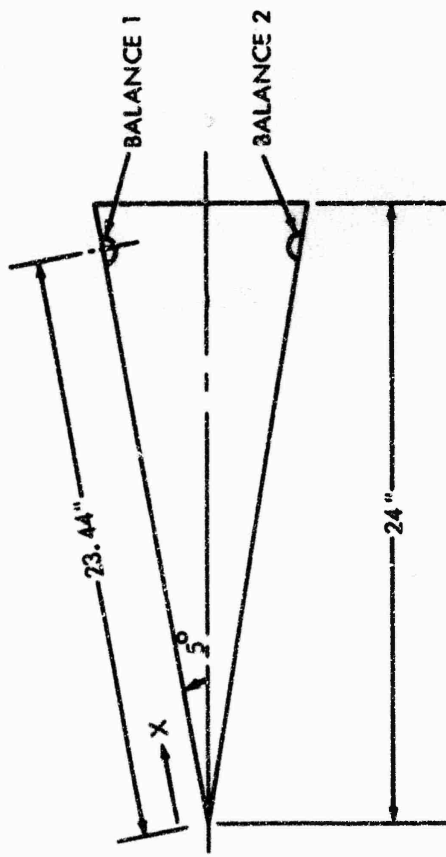
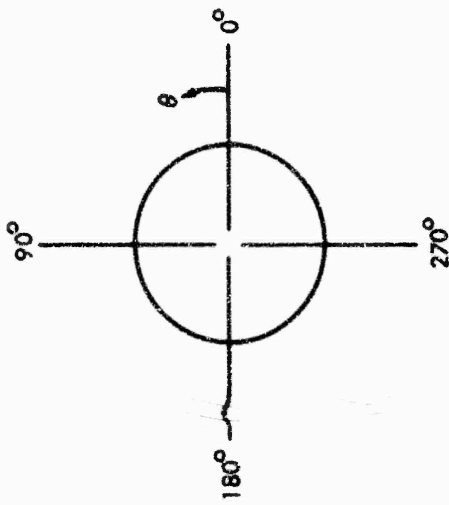


FIG. 1 (U) SCHEMATIC OF THE MODEL (U)



UNCLASSIFIED

UNCLASSIFIED
NOLTR 73-108

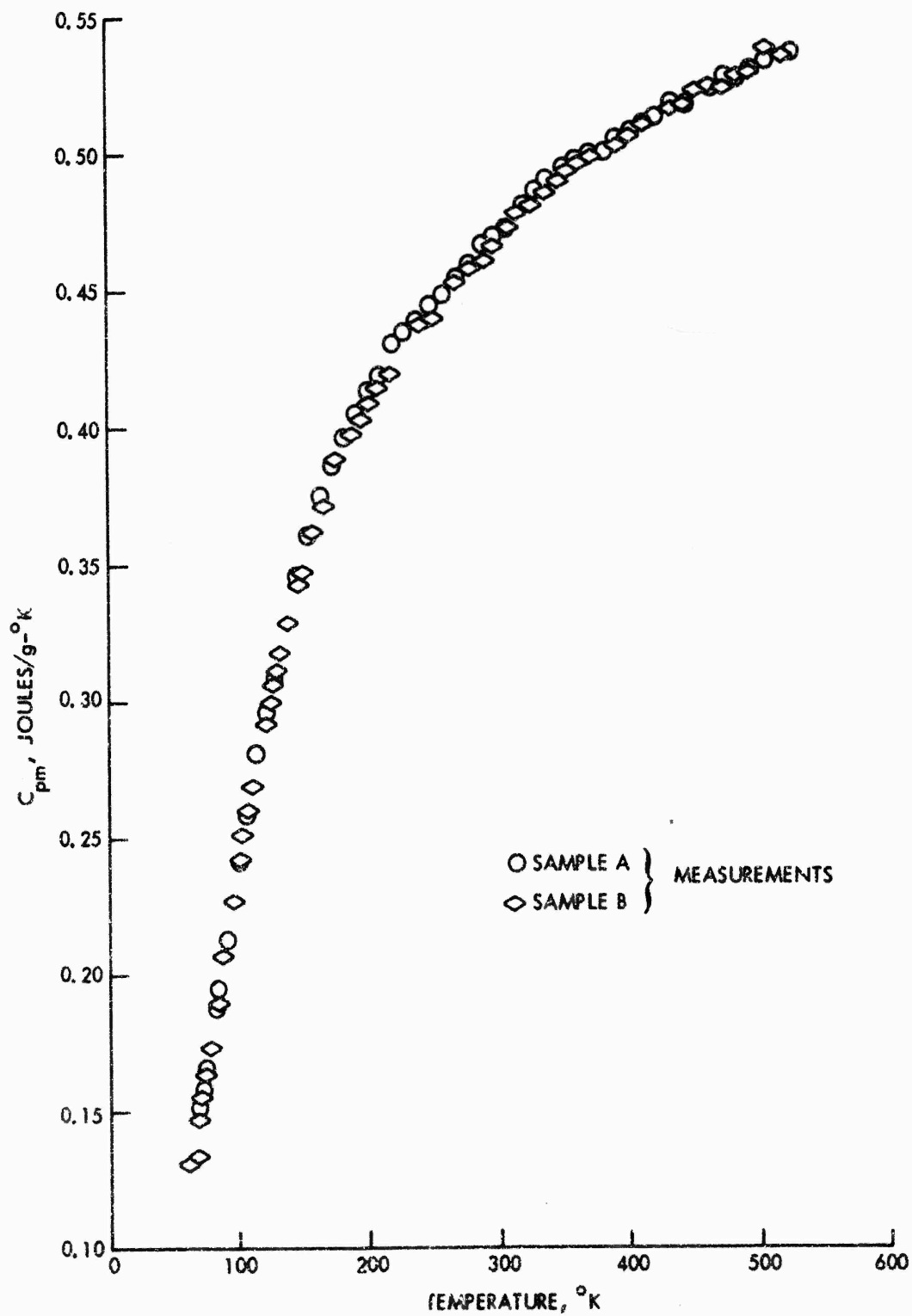


FIG. 2 (U) CONSTANT-PRESSURE SPECIFIC HEAT CAPACITY OF
ARMCO 17-4 PH STAINLESS STEEL (U)

UNCLASSIFIED
NOLTR 73-108

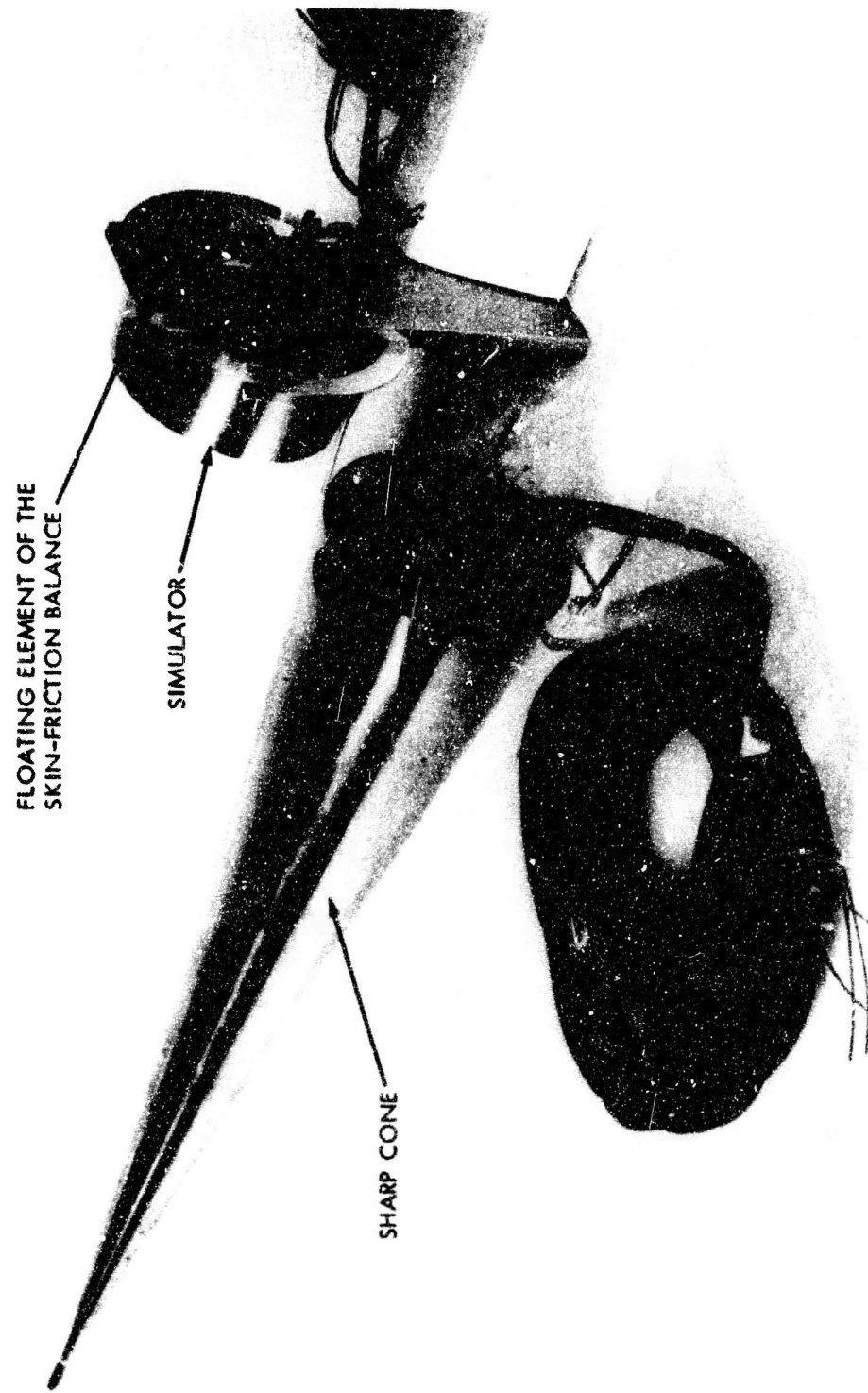


FIG. 3a (U) SKIN-FRICTION BALANCE AND THE MODEL (U)

16
UNCLASSIFIED

UNCLASSIFIED
NOLTR 73-108

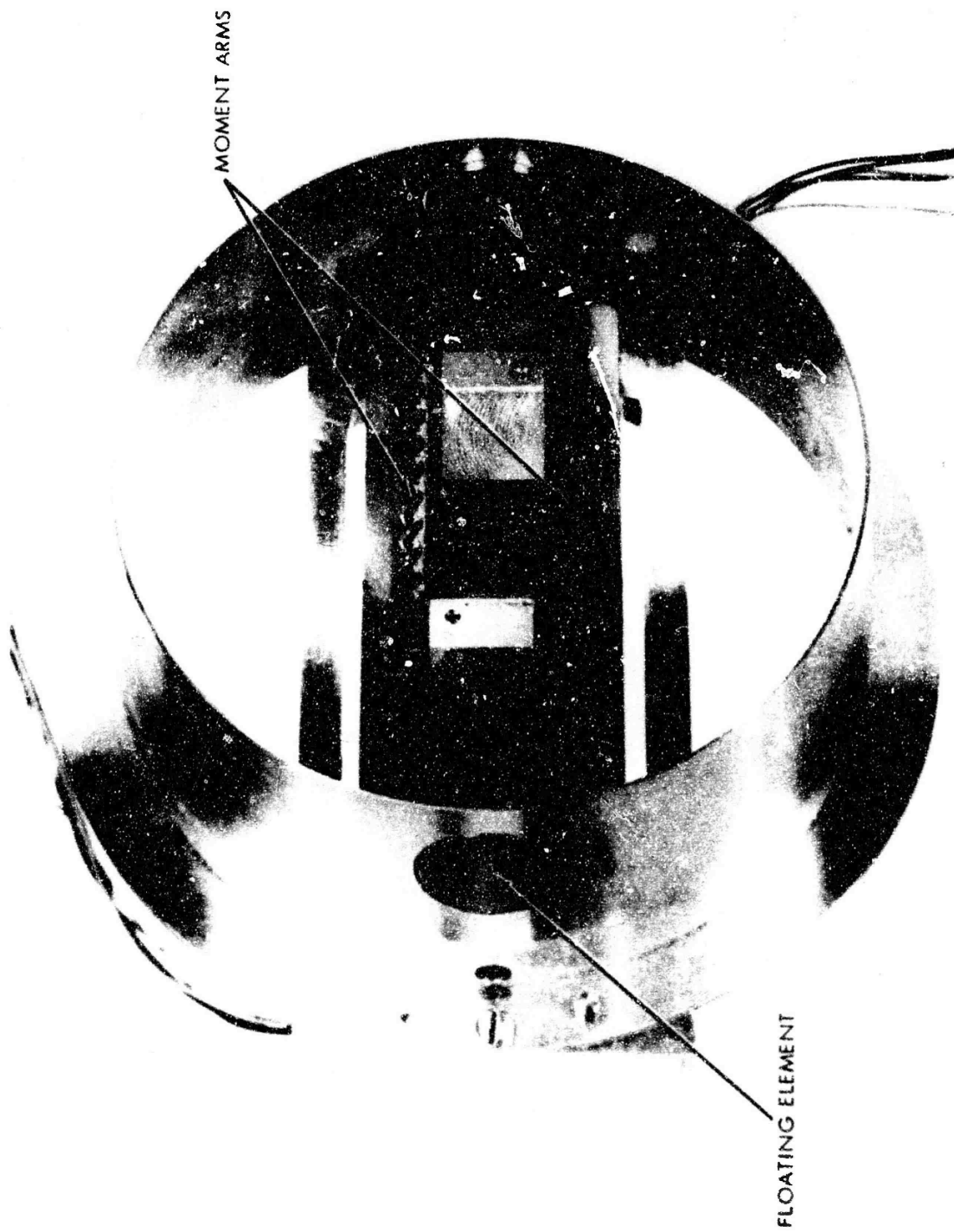


FIG. 3b (U) FRONT VIEW OF THE SKIN-FRCTION BALANCE (U)

Reproduced from
best available copy.

UNCLASSIFIED

UNCLASSIFIED
NOLTR 73-108

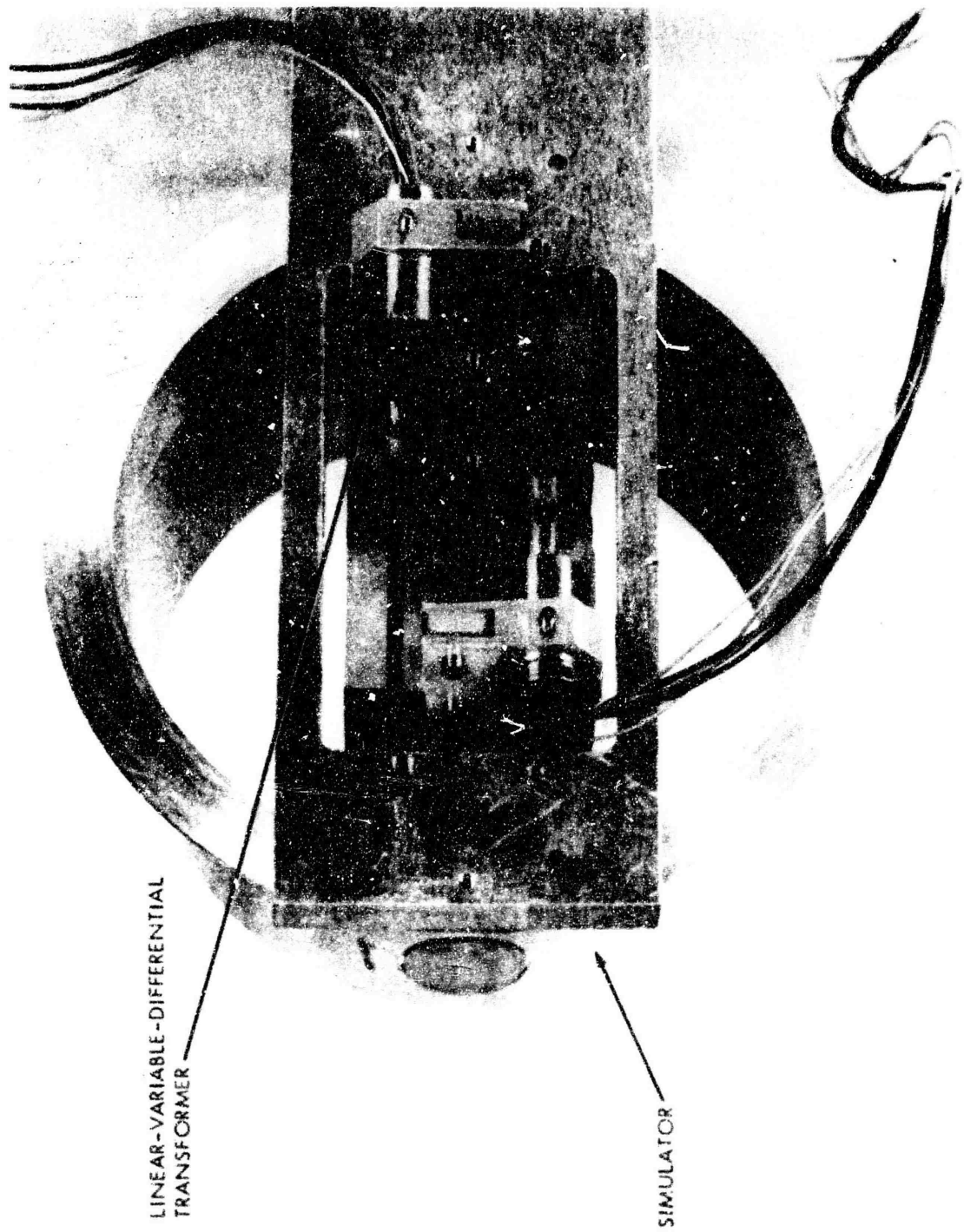


FIG. 3c (U) REAR VIEW OF THE SKIN-FRICTION BALANCE (U)

UNCLASSIFIED

UNCLASSIFIED
NOLTR 73-108

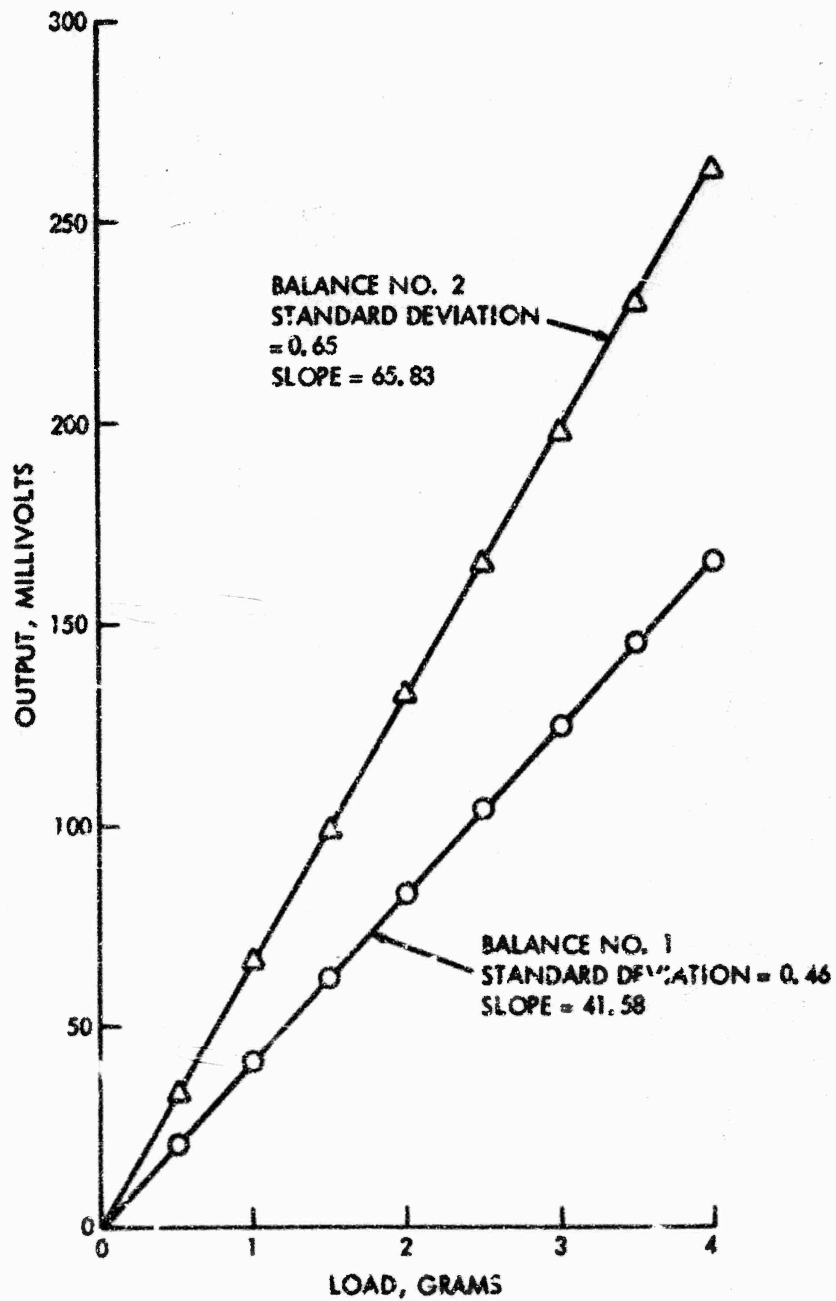


FIG. 4(U) CALIBRATION RESULTS OF SKIN-FRICTION BALANCES (U)

UNCLASSIFIED
NOLTR 73-108

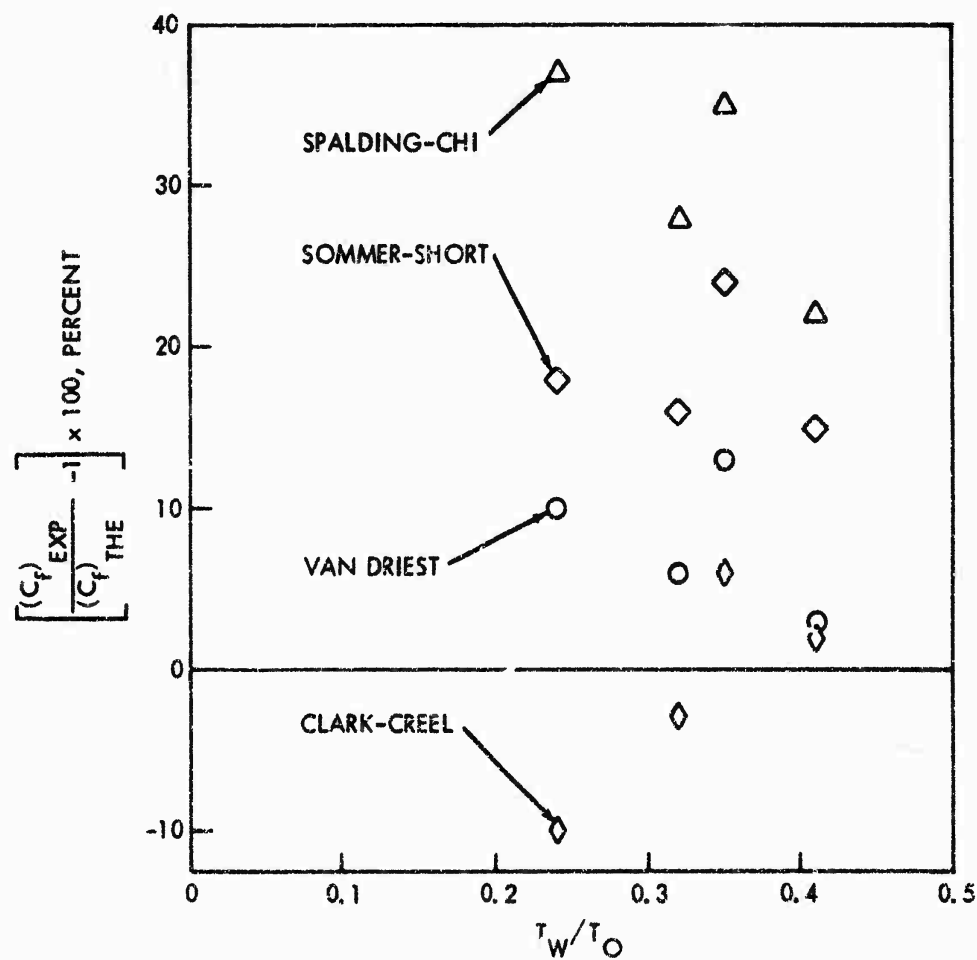


FIG. 5 (U) COMPARISON OF SKIN-FRCTION DATA WITH THEORIES (U)

UNCLASSIFIED

20

UNCLASSIFIED
NOLTR 73-108

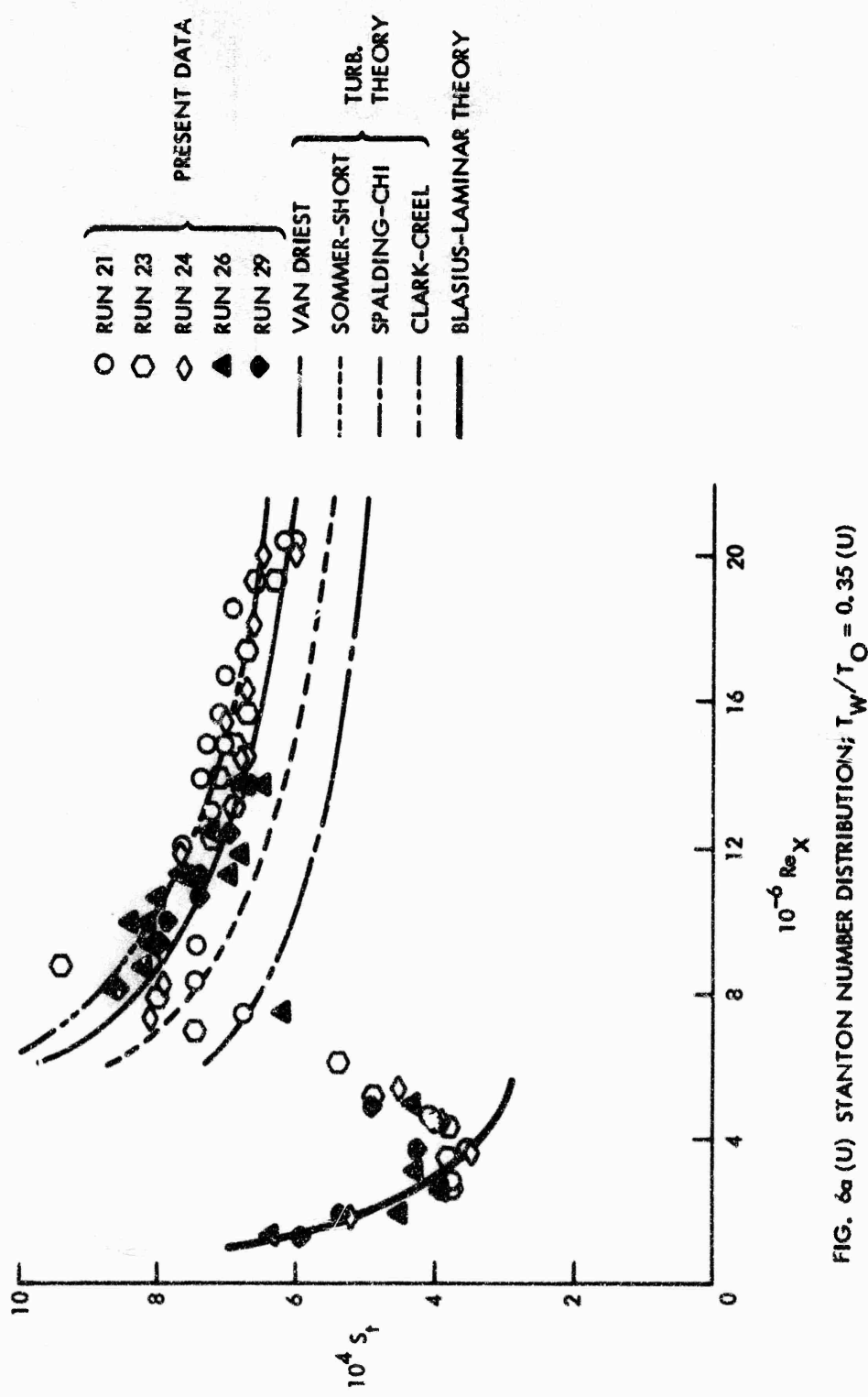


FIG. 6a (U) STANTON NUMBER DISTRIBUTION; $T_w/T_o = 0.35$ (U)

UNCLASSIFIED
NOLTR 73-108

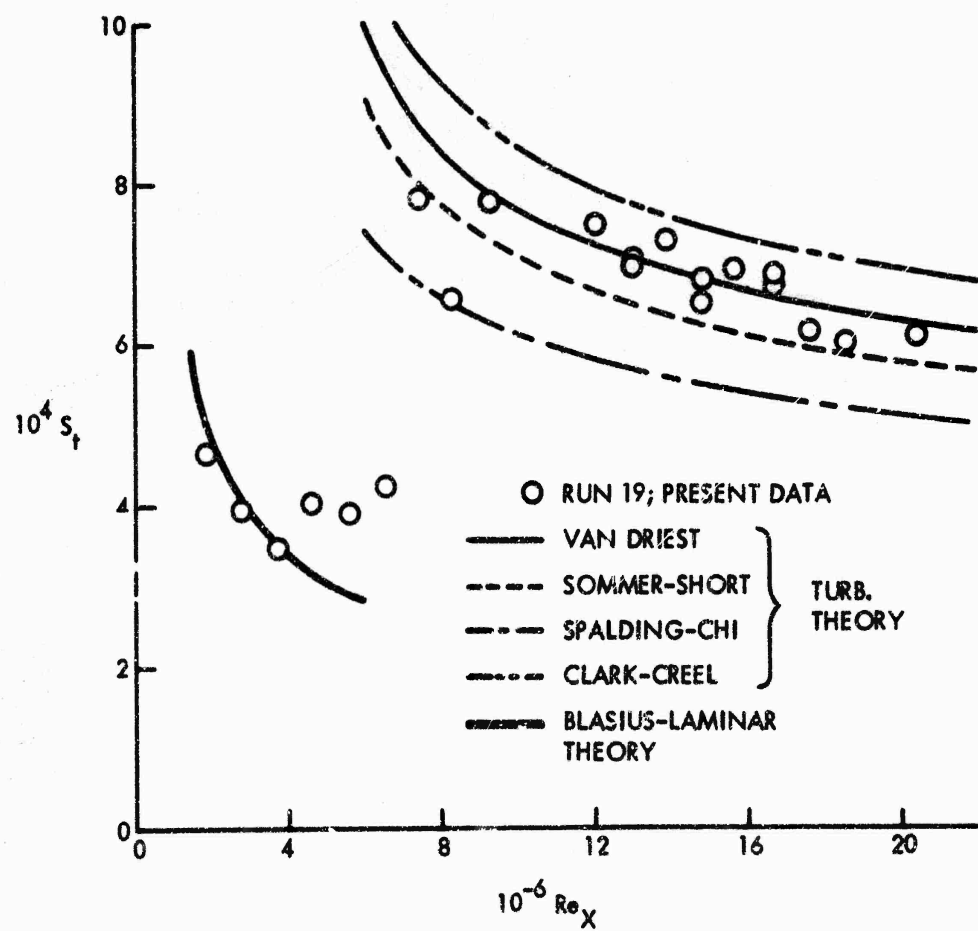


FIG. 6b (U) CONTINUED; $T_w/T_o = 0.32$ (U)

2-2

UNCLASSIFIED

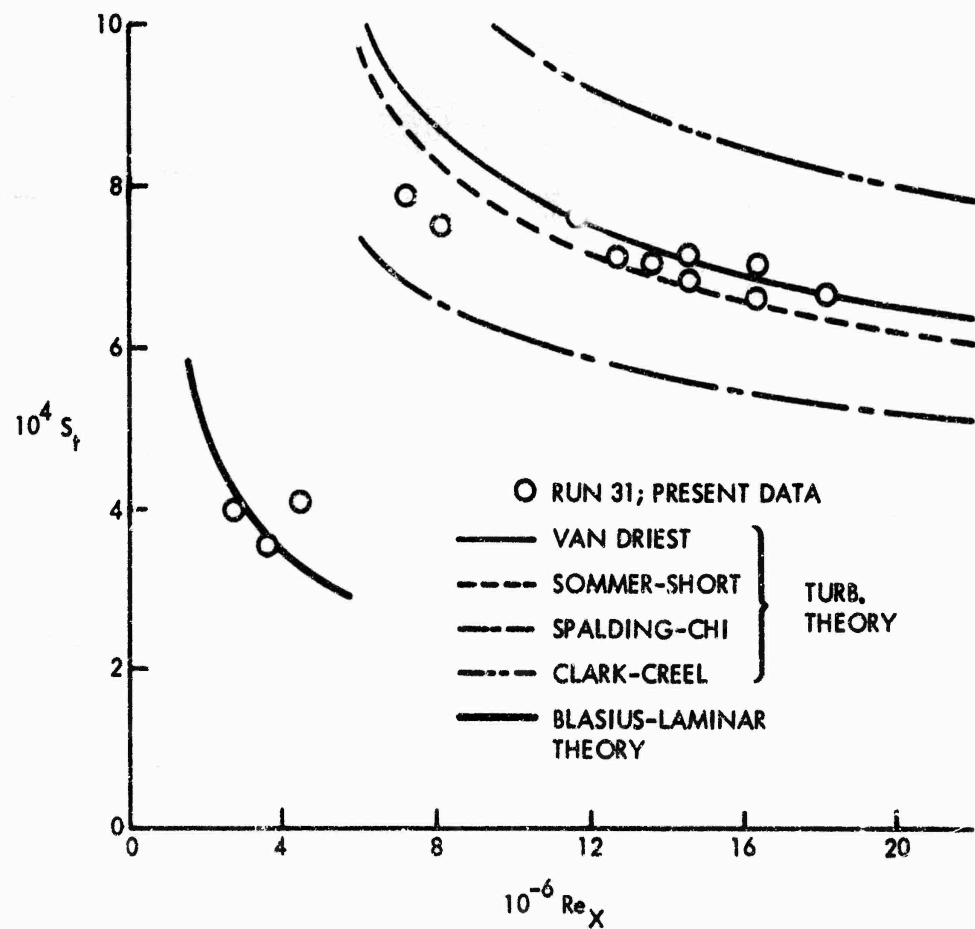


FIG. 6c (U) CONTINUED; $T_w/T_o = 0.24$ (U)

23

UNCLASSIFIED
NOLTR 73-108

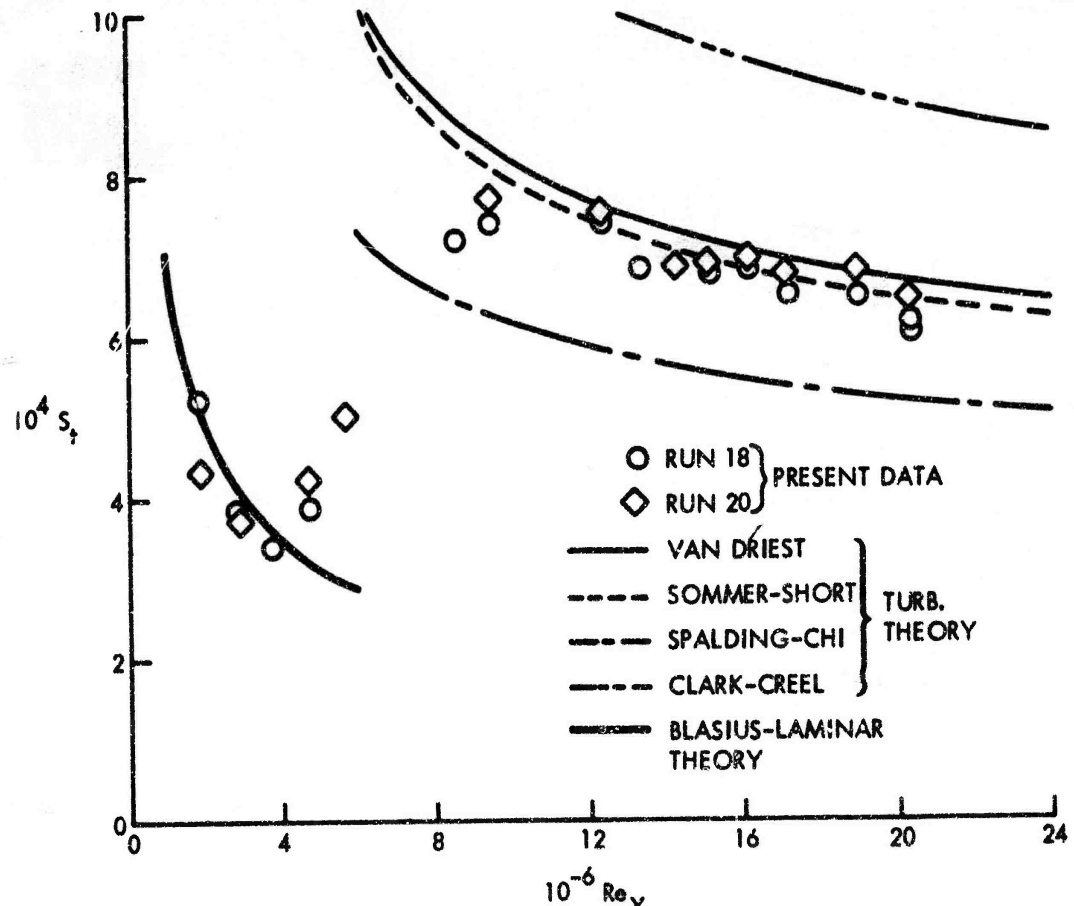


FIG. 6d (U) CONTINUED; $T_w/T_\infty = 0.20$ (U)

24

UNCLASSIFIED

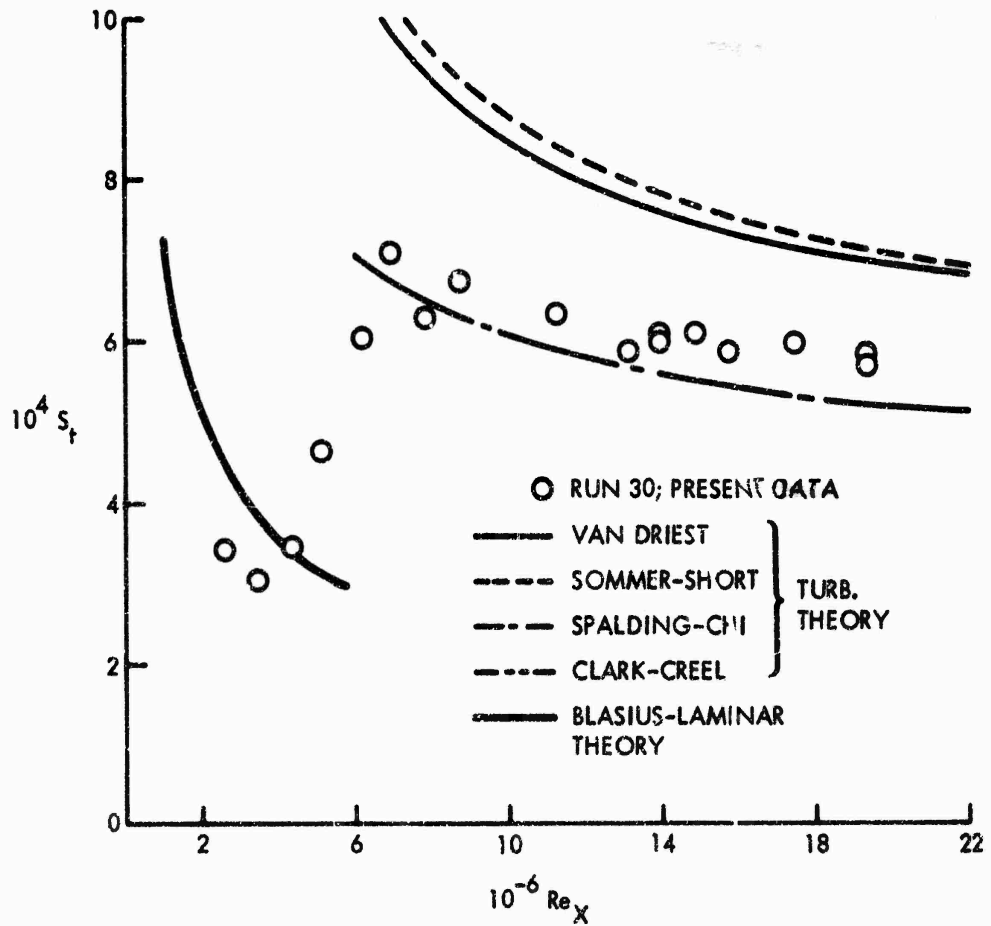


FIG. 6e (U) CONCLUDED; $T_w/T_o = 0.11$ (U)

25

UNCLASSIFIED
NOLTR 73-108

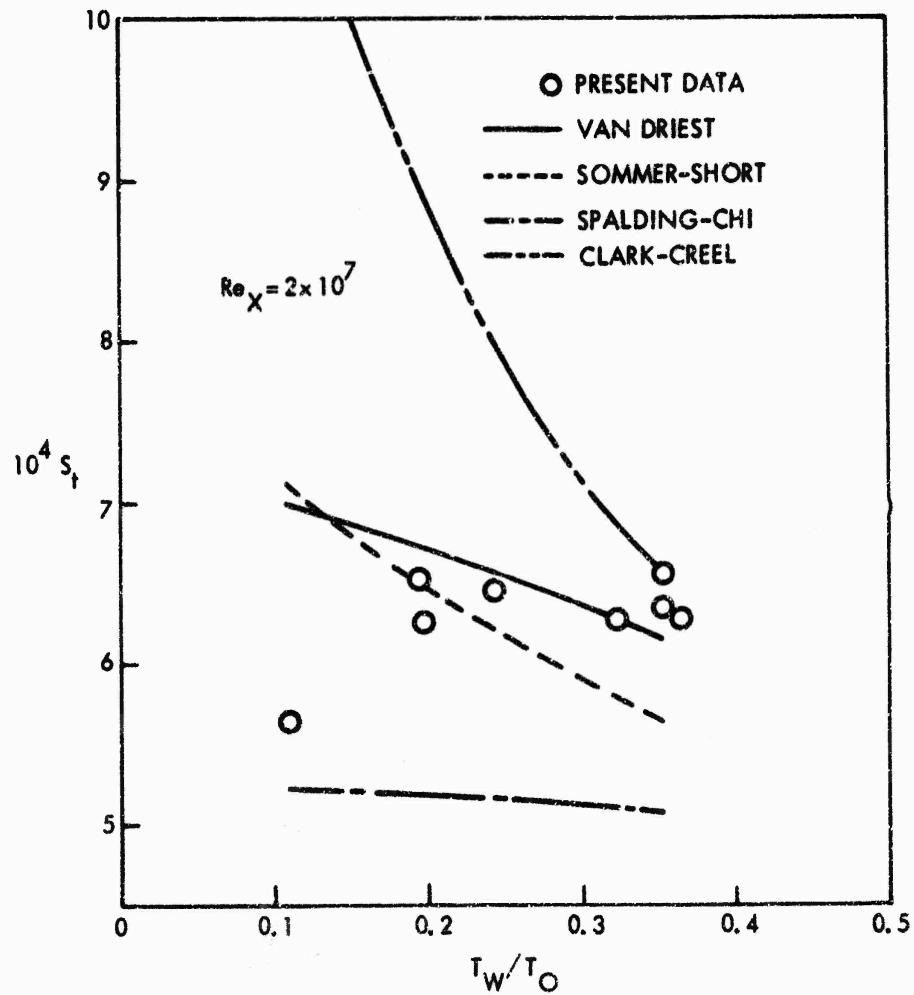


FIG. 7(U) WALL-TEMPERATURE EFFECT ON THE STANTON NUMBER (U)

.26

UNCLASSIFIED

UNCLASSIFIED
NOLTR 73-108

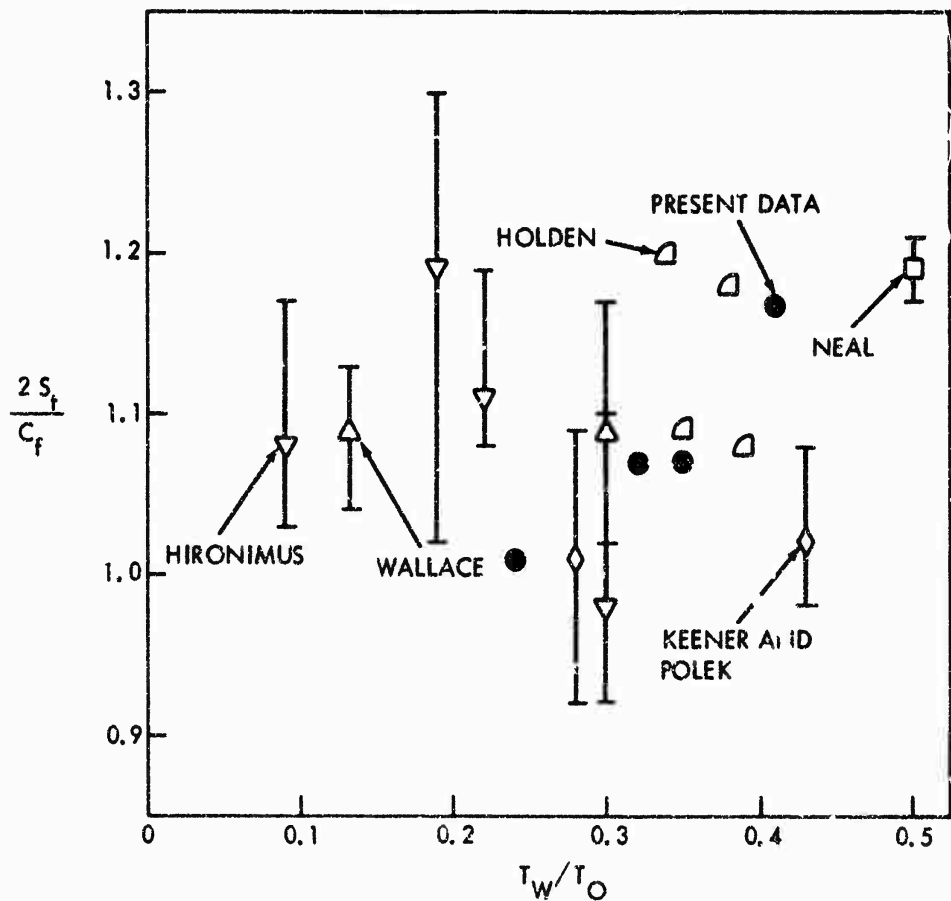


FIG. 8 (U) REYNOLDS ANALOGY FACTOR (U)

27

UNCLASSIFIED